Effect of Closed Shell Structure on Heavy-Ion Fusion Reactions

Hiroshi IKEZOE[1,*], Ken-Ichiro SATOU[1,2], Sinichi MITSUOKA[1], Katsuhisa NISHIO[1], Kaoru TSURUTA[1], Sun-Chang JEONG[3], and Cheng-Jiang LIN[1,4]

[1]*Japan Atomic Energy Research Institute, Tokai, Ibaraki 319-1195, Japan*
[2]*Institute of Physics and Tandem Accelerator Center, University of Tsukuba, Tsukuba-shi, Ibaraki 305-8577, Japan*
[3]*Institute of Particle and Nuclear Studies, KEK, Tsukuba-shi, Ibaraki 305-0801, Japan*
[4]*China Institute of Atomic Energy, P.O. Box 275(10), Beijing 102413, P. R. China*

The effect of the nuclear shell structure on the heavy-ion fusion reaction was investigated for the reaction systems ^{82}Se + ^{138}Ba, ^{82}Se + ^{134}Ba, ^{16}O + ^{204}Pb, ^{86}Kr + ^{134}Ba, ^{86}Kr + ^{138}Ba, and ^{82}Se + $^{nat.}$Ce. Evaporation residues for these fusion reactions were measured using a recoil mass separator (JAERI-RMS) near Coulomb barrier region. The measured evaporation residue cross sections for the reactions ^{82}Se + ^{138}Ba and ^{86}Kr + ^{138}Ba were two orders of magnitude and one order of magnitude larger than those for the reactions ^{82}Se + ^{134}Ba and ^{86}Kr + ^{134}Ba, respectively, at the excitation energy region of 10 $\sim$ 30 MeV. The evaporation residue cross sections were compared with those of the other reaction systems that make the same or similar compound nuclei as the present reaction systems. It was found that the evaporation residue cross sections correlate strongly with the sum of the shell energies for both projectile and target nuclei, i.e., the evaporation residue cross sections increase as the sum of the shell energy decreases.

§1. Introduction

Fusion process between heavy nuclei to produce super-heavy elements has been extensively investigated so far. It is well known that the fusion probability between heavy nuclei is sensitive to the product Z_pZ_t of the atomic numbers of projectile and target, i.e., the Coulomb repulsion at contact. When the charge product is less than $\sim$1800, its fusion cross section is well reproduced by the conventional one-dimensional barrier penetration model. When the charge product is larger than $\sim$1800, its fusion cross section is considerably reduced compared with the model calculation. This fact means that interacting nuclei cannot always fuse to make a compound nucleus even if they have an enough kinetic energy to surmount the fusion barrier between two nuclei. This is because the saddle point of heavy compound nucleus is more compact than a touching configuration of two nuclei. An extra kinetic energy is needed so that the reaction system can reach the saddle point after surmounting the fusion barrier. This extra kinetic energy begins to increase sharply at the charge product $\sim$1800.[1)]

A fusion probability between heavy nuclei at a low excitation energy is sensitive to not only the charge product Z_pZ_t but also the nuclear structure of projectile and target. It has been reported that the number of a valence nucleon outside a major

*) E-mail: ikezoe@popsvr.tokai.jaeri.go.jp

shell changes the fusion probability,[1),2)] i.e., the extra kinetic energy increases as the number of the valence nucleon. This effect was incorporated as a small correction in the systematics of the extra kinetic energy.[1)] A large deviation from this systematics has been reported by Oganessian et al.,[3)] where they found a large difference in the evaporation residue cross sections between the fusion reactions ^{136}Xe + ^{86}Kr and ^{130}Xe + ^{86}Kr, where the nucleus ^{136}Xe has a closed neutron shell $N = 82$ and the neutron number of the nucleus ^{130}Xe is 76. The measured evaporation residue cross sections for the fusion reaction ^{136}Xe + ^{86}Kr are almost two to three orders of magnitude larger than those for the fusion reaction ^{130}Xe + ^{86}Kr near the Coulomb barrier region. This large difference can not be ascribed to the decay property of the two compound nuclei ^{222}Th and ^{216}Th in their de-excitation processes. The enhancement of the evaporation residue cross sections for the fusion reaction ^{48}Ca + ^{208}Pb is also pointed out in Ref. 4). Recently, We reported the measurements of the evaporation residue cross sections for the reactions ^{82}Se + ^{138}Ba and ^{82}Se + ^{134}Ba, where the nucleus ^{138}Ba has a closed neutron shell of $N = 82$ and the nucleus ^{134}Ba has a neutron muber of 78. We showed that the measured evaporation residue cross section for the reaction ^{82}Se + ^{138}Ba was two orders of magnitude larger than those for the reaction ^{82}Se + ^{134}Ba.[5)] This large difference could not be explained by the decay properties for the compound nuclei ^{220}Th and ^{216}Th, and is rather ascribed to the fusion process itself.

In this paper, we report the experimental results on the fusion reactions ^{86}Kr + ^{134}Ba, ^{86}Kr + ^{138}Ba and ^{82}Se + $^{\text{nat.}}$Ce, where the nucleus ^{86}Kr has the closed neutron shell $N = 50$. The nucleus $^{\text{nat.}}$Ce consists of the isotope ^{140}Ce with the natural abundance of 88.48%, which has the closed neutron shell $N = 82$. Recently, Hinde et al.[6)] showed that the cross sections of the evaporation residues for the reaction system ^{16}O + ^{204}Pb, which makes the compound nucleus ^{220}Th, is one order of magnitude larger than that of the reaction system ^{82}Se + ^{138}Ba. In order to verify this fact, we also measured the evaporation residues for the reaction ^{16}O + ^{204}Pb. Based on these experimental results, we emphasize that the sum of the shell energy of projectile and target are important quantities having a strong effect on the heavy-ion fusion process.

§2. Experimental procedures

Evaporation residues for the fusion reactions ^{86}Kr + ^{138}Ba, ^{86}Kr + ^{134}Ba and ^{82}Se + $^{\text{nat.}}$Ce were measured using ^{86}Kr and ^{82}Se beams from JAERI-tandem booster accelerator and the JAERI-recoil mass separator (JAERI-RMS).[7)] The detailes of the experimental procedures are written in Ref. 9).

As for the measurements of the evaporation residues produced for the reaction ^{16}O + ^{204}Pb, the evaporation residues recoiling out from a target foil were implanted in an aluminum catcher foil. After the irradiation of 70 to 90 min. by ^{16}O beams, the catcher foil was put on a silicon surface barrier detector to detect subsequent α-decays from implanted evaporation residues.

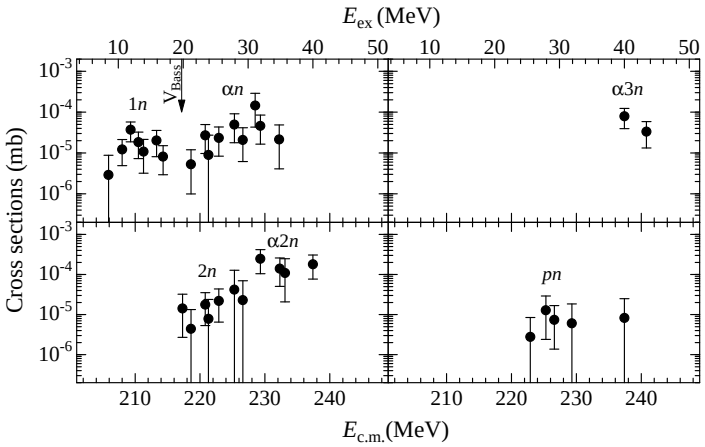

Fig. 1. Evaporation residue cross sections measured for the reaction ^{86}Kr +^{138}Ba. The arrow indicates the position of the Bass barrier.

§3. Experimental results and discussions

The obtained evaporation residue cross sections for the reaction system ^{86}Kr + ^{138}Ba are plotted in Fig. 1 as a function of *c.m.* energy. Evaporation channels expected in respective energy regions are indicated in the figure. The evaporation residues corresponding to the $3n$ and $4n$ channels were not identified because the half-lives and the α-decay energies for the evaporation residues ^{220}U and ^{221}U were unknown. The $1n$ channel is clearly seen at about 10 MeV below the Bass barrier 217.2 MeV. This means that the actual fusion barrier is extended to a lower energy than the Bass barrier.

The reduced cross sections $\sigma(\mathrm{ER})k^2/\pi$ obtained from the sum of the detected evaporation residues ($1n$, $2n$, αn, $\alpha 2n$, $\alpha 3n$ and pn channels) were plotted in Fig. 2 together with those for other reaction systems which makes the same or the similar compound nuclei ^{222,226,228}U as the present reaction system ^{86}Kr + ^{138}Ba. Here k is the wave number. The measured evaporation residue cross sections for the reactions ^{86}Kr + ^{134}Ba and ^{82}Se + $^{\mathrm{nat.}}$Ce are also plotted for comparison. In the reaction ^{86}Kr + ^{134}Ba, one event corresponding to the αn channel was detected at the excitation energy E_{ex} =29.9 MeV and one event corresponding to the pn channel was detected at each excitation energy of 25.4 MeV and 31.5 MeV. The measurements at E_{ex} = 18.5 MeV and 21.1 MeV correponding to the $1n$ channel were carried out. No evaporation residue was detected at these excitation energies. As for the reaction ^{82}Se + $^{nat.}$Ce, no evaporation residue was observed at E_{ex} = 15.4 MeV, 19.4 MeV and 21.7 MeV.

As shown in Fig. 2, the reduced cross sections for the reaction ^{86}Kr + ^{138}Ba show the largest values among the reaction systems shown at the excitation energy region less than 35 MeV. Above the excitation energy of 35 MeV, the reduced cross section for the reaction system ^{20}Ne + ^{208}Pb[17] becomes largest. This is simply because the charge product $Z_{\mathrm{p}}Z_{\mathrm{t}}$ = 820 is well below the threshold value 1800. It

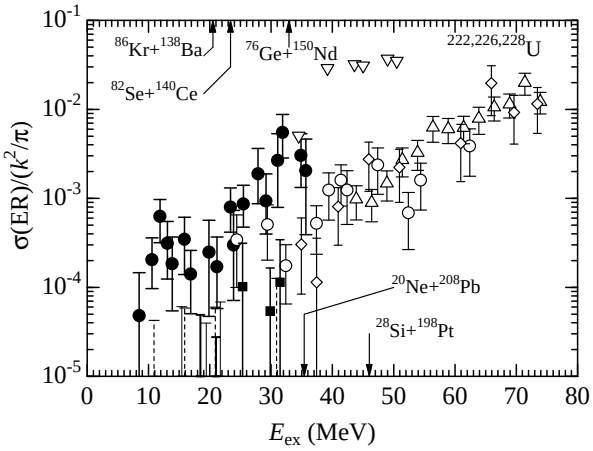

Fig. 2. Reduced evaporation residue cross sections for various reactions; ^{86}Kr + ^{138}Ba (solid circles), ^{86}Kr + ^{134}Ba (solid squares), ^{82}Se + $^{nat.}$Ce (open circles), ^{76}Ge + ^{150}Nd (diamonds[16]), ^{28}Si + ^{198}Pt (open triangles[16]), ^{20}Ne + ^{208}Pb (inverted open triangles[17]). The Bass barriers for these reaction systems are shown as arrows. The Bass barrier for the reaction system ^{86}Kr + ^{134}Ba locates at the excitation energy of 22.7 MeV. The upper limits of the cross section for the reaction systems ^{86}Kr + ^{134}Ba, ^{82}Se + $^{nat.}$Ce and ^{76}Ge + ^{150}Nd are shown as the vertical thick lines , thin lines, and dashed lines with bar, respectively.

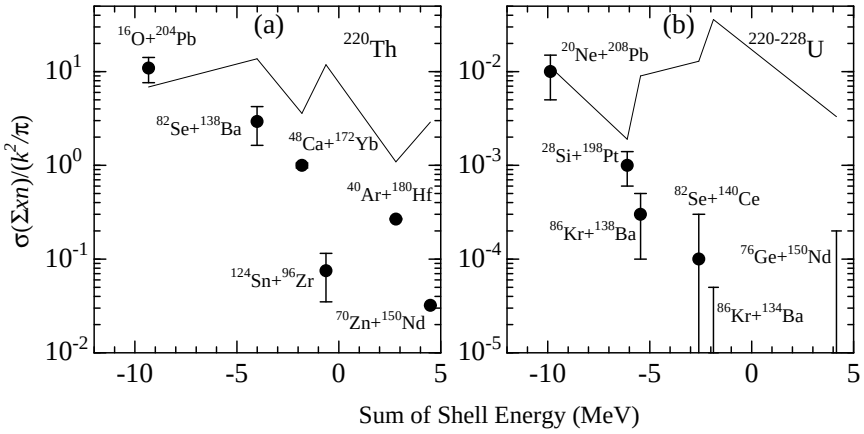

Fig. 3. Reduced evaporation residue cross sections at the Bass barriers as a function of the sum of the shell energy of projectile and target nuclei for various reaction systems. The thin lines show the values calculated by HIVAP.[11]

is noted that although the charge product for the reaction system ^{86}Kr + ^{138}Ba is the largest ($Z_pZ_t = 2016$) among the reaction systems shown here and also well above the threshold value ~ 1800, we observed the $1n$ channel only in this reaction system ^{86}Kr + ^{138}Ba. This result suggests that the fusion of heavy nuclei is not always governed only by the single quantity Z_pZ_t, but also the nuclear structure of interacting nuclei. In order to emphasize this point, the reduced evaporation residue cross sections at the *c.m.* energy corresponding to the Bass barriers are plotted in

Fig. 3(b) as a function of the sum of the shell energy for the projectile and target nuclei.

The shell energy ($M_{\rm exp} - M_{\rm LD}$) was obtained from the mass table of Ref. 10), where $M_{\rm exp}$ and $M_{\rm LD}$ are the experimental mass and the liquid drop mass, respectively. The reduced evaporation residue cross sections at the Bass barriers may depend on the property of each compound nucleus with a different excitation energy and a different mass number. This was simulated using the statistical model code HIVAP.[11] The thin line shows the result of the calculation, where we adopted the statistical mode parameters used in Ref. 9). The calculated values for the evaporation residue cross section do not follow the observed trend as a function of the sum of the shell energy. On the other hand, the measured evaporation residue cross sections increase smoothly as the sum of the shell energy decreases in negative values. This result indicates that the sum of the shell energy is an important quantity for the formation of the compound nucleus.

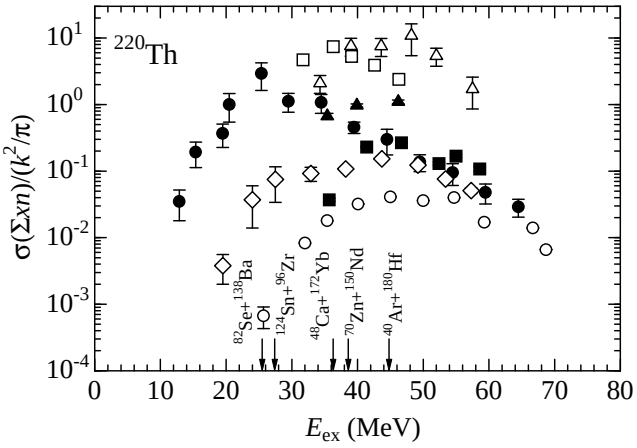

Fig. 4. Reduced evaporation residue cross sections for various reaction systems which make the compound nucleus ^{220}Th; ^{82}Se + ^{138}Ba (solid circles[5]), ^{48}Ca + ^{172}Yb (solid triangles[18]) , ^{40}Ar + ^{180}Hf (solid squares[19]), ^{124}Sn + ^{96}Zr (diamonds[19]), ^{70}Zn + ^{150}Nd (open circles[22]), ^{16}O + ^{204}Pb (open triangles for the present work and open squares of Ref. 6)). The positions of the Bass barriers for these reaction systems are indicated by the arrows. The Bass barrier for the reaction system ^{16}O + ^{204}Pb locates at $E_{\rm ex} = 31.1$ MeV.

In Fig. 4, we plotted the reduced cross sections $\sigma(\Sigma xn)k^2/\pi$ for the various reaction systems which make the compound nucleus ^{220}Th. Here, $\sigma(\Sigma xn)$ is the sum of the observed xn channels ($x = 1$ to 7). Our previous data for the reaction ^{82}Se + ^{138}Ba[5] and the present data for the reaction ^{16}O + ^{204}Pb are also included together with the data of Ref. 9). We see that the reduced cross section for the reaction ^{82}Se + ^{138}Ba shows a peak exactly at the Bass barrier of this reaction system. The present result shows no fusion barrier shift and a narrow barrier distribution centered at the Bass barrier. On the other hand, the absolute values of the reduced cross section for the reaction ^{82}Se + ^{138}Ba is the one order of magnitude smaller than that for the fusion reaction ^{16}O + ^{204}Pb. This point will be discussed later.

The reaction systems ^{124}Sn + ^{96}Zr and ^{70}Zn + ^{150}Nd show a broad barrier

distribution extended from their Bass barrier energies to the energies larger by about 20 MeV than the Bass barriers. These broad barrier distributions are commonly observed in the heavy-ion fusion reaction as shown in Ref. 1) and well correlated with the extra kinetic energy needed for fusion. This systematics[1)] is not true for the reaction ^{82}Se + ^{138}Ba. We expect the extra kinetic energy around $10 \sim 15$ MeV for the reaction ^{82}Se + ^{138}Ba based on this systematics. This effectively makes the fusion barrier high and considerably decreases the $1n$ and $2n$ channels cross-sections at the low excitation energy region less than 30 MeV. There is no barrier shift seen in Fig. 4. On the other hand, the reduced evaporation residue cross section for the reaction ^{82}Se + ^{134}Ba[5)] shows the consistent trend as predicted by the systematics,[1)] i.e., the fusion barrier is shifted to a high energy by the amount of $10 \sim 15$ MeV.[5),12)]

Our present data for the evaporation residue cross section in the reaction ^{16}O + ^{204}Pb are consistent with and even larger than those of Hinde et al.[6)] If we assume no fusion hindrance for the reaction ^{16}O + ^{204}Pb, the present result shows that the fusion for the reaction ^{82}Se + ^{138}Ba is hindered by the one order of magnitude or more at the energy region above the Bass barrier. This hindrance can be ascribed to the formation process of the compound nucleus after soumounting the fusion barrier. We plotted the relative positions between the saddle point of the compound nucleus ^{220}Th and the contact points for various reaction systems in Fig. 5. Here, the abscissa shows the distance between the mass centers for two touching spherical nuclei and the ordinate shows the effective fissility parameter x_{eff}. Here, R_0 is the radius of the compound nucleus ^{220}Th. The position of the saddle point of ^{220}Th predicted by Ref. 20) is also indicated by the thin line. The parameter x_{eff} is a measure for the ratio of Coulomb repulsion to nuclear attraction at half-density overlap.[21)] As shown in Fig. 5, the contact points for the reaction systems except the system ^{16}O + ^{204}Pb locate close to or outside the saddle point and their effective fissility parameters are larger than that for the reaction system ^{16}O + ^{204}Pb. This suggests qualitatively that in the fusion process after surmounting the Coulomb barrier, the reaction system ^{16}O + ^{204}Pb forms more easily the compound nucleus than the other reaction systems. In order to verify this suggestion quantitatively, a theoretical calculation taking into account the dynamics on a multi-dimensional potential energy surface is needed.

In Fig. 3(a), we plotted the reduced cross sections at the Bass barriers for various reaction systems which make the compound nucleus ^{220}Th. The reduced evaporation residue cross sections are not totally correlated with the excitation energy of the compound nucleus and rather well correlated with the sum of the shell energy of the target and projectile nuclei. It is clearly seen that the reduced cross section increases as the sum of the shell energies decreases in negative values, i.e., the target and/or projectile with a closed shell structure makes the fusion probability high. This systematic trend is consistent with that seen in Fig. 3(b).

Myers and Swiatecki[13)] pointed out that the shell energy resists neck growth at the time of contact between projectile and target, and then the projectile nucleus can approaches closely to the target nucleus with a small kinetic energy dissipation. They proposed the sum of the shell energy and the congruence energy for both projectile and target as a resistance factor against the neck growth. The observed trend seen in Fig. 3(a) and 3(b) is essentially unchanged even if the reduced evaporation residue

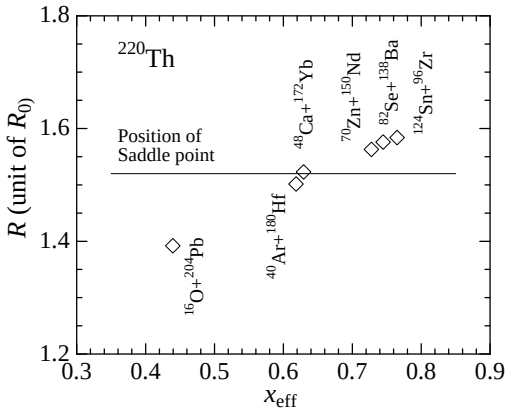

Fig. 5. Positions of contact points (diamonds) for various reaction systems. The position of the saddle point of the nucleus ^{220}Th is indicated by the horizontal thin line.

cross section is plotted as a function of the sum of the shell energy and the congruence energy. Therefore, the present data are consistent with this argument.

Möller and Sierk discussed the fusion process on the multi-dimensional microscopic potential energy surface.[14] When heavy nuclei first touch, mainly the Coulomb repulsive force push the system to deformations and eventually the system falls down the fission valley. If the system resists deformations away from the fusion path by the help of the shell energy, the system may proceed to a compound nucleus following the fusion path. This argument qualitatively explains the present data. Oganessian et al. suggests the close relation between the fusion process and the fission process.[3] In the case of the fusion reaction ^{136}Xe + ^{86}Kr, the low excited compound nucleus ^{222}Th can decay into the asymmetric fission components close to the nuclei ^{86}Kr and ^{136}Xe. The compound nucleus ^{220}Th which is produced in the fusion reaction ^{82}Se + ^{138}Ba, may decay into the asymmetric fission components close to the nuclei ^{82}Se and ^{138}Ba.[15] On the other hand, the compound nucleus ^{216}Th, which is formed in the fusion reactions ^{130}Xe + ^{86}Kr and also ^{82}Se + ^{134}Ba, has little chance to decay into such asymmetric fission component.[15] This argument is also related to the shell structure of final fragments. We conclude that the shell energy of the projectile and target plays a major role in the fusion process between heavy nuclei in addition to the Coulomb repulsive force characterized as the quantity $Z_{\rm p}Z_{\rm t}$.

§4. Summary and conclusions

Evaporation residues for the reactions ^{82}Se + ^{138}Ba, ^{82}Se + ^{134}Ba, ^{16}O + ^{204}Pb, ^{86}Kr + ^{138}Ba, ^{86}Kr + ^{134}Ba and ^{82}Se + $^{\rm nat.}$Ce were measured to investigate the fusion process. The evaporation residue cross sections measured in the reactions ^{82}Se + ^{138}Ba and ^{86}Kr + ^{138}Ba were almost two orders of magnitude and one order of magnitude larger near the Coulomb barrier region than those for the reactions ^{82}Se + ^{134}Ba and ^{86}Kr + ^{134}Ba, respectively. These large differences are ascribed to

the entrance channel property of the fusion process. The present data were compared with the other reaction systems, which make the same or similar compound nuclei as the present reactions. From these comparisons, we conclude that the fusion for massive reaction systems is strongly affected by the shell structure of colliding nuclei in addition to the Coulomb repulsion $Z_{\rm p}Z_{\rm t}$. It is important to realize theoretically the energy dissipation due to the friction after contact by taking into account the shell structure of projectile and target nuclei. Further experimental investigation is needed also to make the relation between fusion and fission clear.

Acknowledgements

We would like to thank the crew of the JAERI tandem booster facility for the beam operation.

References

1) A. B. Quint, W. Reisdorf, K.-H. Schmidt, P. Armbruster, F. P. Hessberger, S. Hofmann, J. Keller, G. Müzenberg, H. Stelzer, H.-G. Clerc, W. Morawek, and C.-C. Sahm, Z. Phys. A **346** (1993), 119.
2) K.-H. Schmidt and W. Morawek, Rep. Prog. Phys. **54** (1991), 949.
3) Yu Ts. Oganessian, *Heavy Elements and Related New Phenomena*, edited by W. Greiner and R. K. Gupta (World Scientific, 1999), Vol.1, p. 43.
4) Yu Ts. Oganessian, V. K. Utyonkov, Yu. V. Lobanov, F. S. Abdullin, A. N. Polyakov, I. V. Shirokovsky, Yu S. Tsyganov, A. N. Mezentsev, S. Iliev, V. G. Subbotin, A. M. Sukhov, K. Subotic, O. V. Ivanov, A. N. Voinov, V. I. Zagrebaev, K. J. Moody, J. F. Wild, N. J. Stoyer, M. A. Stoyer and R. W. Lougheed, Phys. Rev. C **64** (2001), 054606.
5) K. Satou, H. Ikezoe, S. Mitsuoka, K. Nishio and S. C. Jeong, Phys. Rev. C **65** (2002), 054602.
6) D. J. Hinde, M. Dasgupta and A. Mukherjee, Phys. Rev. Lett. **89** (2002), 282701.
7) H. Ikezoe, Y. Nagame, T. Ikuta, S. Hamada, I. Nishinaka and T. Ohtsuki, Nucl. Instrum. Methods, A **376** (1996), 420.
8) R. B. Firestone, *Table of Isotopes*, edited by V. S. Shirley (Wiley, New York, 1996).
9) S. Mitsuoka, H. Ikezoe, K. Nishio and J. Lu, Phys. Rev. C **62** (2000), 054603.
10) W. D. Myers and W. J. Światecki, Nucl. Phys. **A601** (1996), 141.
11) W. Reisdorf and M. Schädel, Z. Phys. A **343** (1992), 47.
12) H. Ikezoe, K. Satou, S. Mitsuoka, K. Nishio and S. C. Jeong, Phys. Atom. Nucl. **66** (2003), 1053.
13) W. D. Myers and W. J. Światecki, Phys. Rev. C **62** (2000), 044610.
14) P. Möller and A. J. Sierk, Nature Vol. **422** (2003), 485.
15) K.-H. Schmidt, S. Steinhäuser, C. Böckstiegel, A. Grewe, A. Heinz, A. R. Junghans, J. Benlliure, H.-G. Clerc, M. de Jong, J. Müller, M. Pfützner and B. Voss, Nucl. Phys. **A665** (2000), 221.
16) K. Nishio, H. Ikezoe, S. Mitsuoka and J. Lu, Phys. Rev. C **62** (2000), 014602.
17) R. N. Sagaidak, V. I. Chepigin, A. P. Kabachenko, J. Roháč, Yu. Ts. Oganessian, A. G. Popeko, A. V. Yeremin, Ans. D'Arrigo, G. Fazio, G. Giardina, M. Herman, R. Ruggeri and R. Sturiale, J. Phys. G: Nucl. Part. Phys. **24** (1998), 611.
18) C.-C. Sahm, H.-G. Clerc, K.-H. Schmidt, W. Reisdorf, P. Arumbruster, F. P. Hessberger, J. G. Keller, G. Münzenberg and D. Vermeulen, Nucl. Phys. **A441** (1985), 316.
19) H.-G. Clerc, J. G. keller, C.-C. Sahm, K.-H. Schmidt, H. Schulte and D. Vermeulen, Nucl. Phys. **A419** (1984), 571.
20) J. R. Nix and A. J. Sierk, Phys. Rev. C **15** (1977), 2072.
21) W. J. Swiatecki, Prog. Part. Nucl. Phys. **4** (1980), 383.
22) C. Stodel, PhD thesis, LPC Caen (1998).